Do Stereochemical Effects Overcome a Charge-induced Perturbation in Isolated Protonated cyclo(Tyr-Tyr)?

Koki Yoshizawa, Keisuke Hirata, Shun-Ichi Ishiuchi, Masaaki Fujii, Anne Zehnacker

Do Stereochemical Effects Overcome a Charge-induced Perturbation in Isolated Protonated cyclo(Tyr-Tyr)?

Koki Yoshizawa,[1,2] Keisuke Hirata,[1,3] Shun-ichi Ishiuchi,[1,3] Masaaki Fujii,[1,2,4*] Anne Zehnacker,[4,5*]

[1]*Laboratory for Chemistry and Life Science, Institute of Innovative Research, Tokyo Institute of Technology, 4259, Nagatsuta-cho, Midori-ku, Yokohama, 226-8503, Japan*

[2]*School of Life Science and Technology, Tokyo Institute of Technology. 4259 Nagatsuta-cho, Midori-ku, Yokohama, Kanagawa, 226-8503, Japan.*

[3]*Department of Chemistry, School of Science, Tokyo Institute of Technology, 2-12-1 Ookayama, Meguro-ku, Tokyo 152-8550, Japan.*

[4]*International Research Frontiers Initiative (IRFI), Institute of Innovative Research, Tokyo Institute of Technology, 4259, Nagatsuta-cho, Midori-ku, Yokohama, Japan*

[5]*Institut des Sciences Moléculaires d'Orsay (ISMO), CNRS, Université Paris-Saclay, F-91405 Orsay, France*

* Corresponding authors : anne.zehnacker-rentien@universite-paris-saclay.fr, mfujii@res.titech.ac.jp

Abstract

The two diastereomers of the protonated diketopiperazine (DKP) dipeptide cyclo(Tyr-Tyr), namely, cyclo(LTyr-LTyr)H^+ and cyclo(LTyr-DTyr)H^+, are studied in a cryogenic ion trap by means of IR photodissociation spectroscopy combined with quantum chemical calculations. The two diastereomers have similar structures, in which one of the ring is folded over the DKP ring and the other one is extended in a *trans* geometry, allowing a strong OH^+…π interaction to take place. This contrasts to the observation of a stacked geometry for neutral cyclo(LTyr-LTyr) only under supersonic expansion conditions that does not exist for cyclo(LTyr-DTyr). In the protonated form, the strength of the OH^+…π interaction is different for the two diastereomers, resulting in a ~ 110 cm^{-1} difference in the $\nu(OH^+)$ frequency and a smaller, but clearly identifiable difference in the protonated amide ν(NH) frequency. Stereochemical effects are therefore still evidenced despite the strong perturbation due to the excess charge.

Introduction

2,5-Diketopiperazine (DKP) peptides are an important class of natural molecules synthetized mainly by bacteria in fungi or marine microorganisms. They result from the self-condensation of two α-amino acids.[1] Their rigid cyclic structure makes them a unique scaffold for the synthesis of innovative drugs.[2] Their cyclic nature also imposes the unusual *cis* conformation of the peptide bond, as shown in Figure 1. In contrast to the peptide backbone, which shows limited conformational mobility,[3-4] the geometry of the substituents is quite flexible, in particular around the C_α-C_β bond. This flexibility results in different possible structures that

depend on several factors, including the nature of the residue, the protonation or aggregation state, the environment such as the solvent in solution or the crystal in the solid state.[5-8 9-11] Two different structures of peptides containing one aromatic residue coexist under jet-cooled conditions: a folded structure, with the aromatic ring folded over the DKP ring, and an extended one with the aromatic ring extended outwards the molecule.[12] The folded structure is stabilised by solvation and is the only form observed in condensed-phase studies.[9-11] It should be noted here that the cyclic nature of the DKP peptide deprives them from both C- and N-termini. Therefore, no zwitterion is observed in the condensed phase. Dipeptides containing two aromatic residues involve both repulsion between the bulky substituents and dispersion interactions. Their structure is therefore dictated by the subtle balance between these different forces. For cyclo(LPhe-LPhe), repulsion dominates and a single conformation exists under jet-cooled conditions, with one of the phenyl substituents folded on the peptide ring and the other extended outwards.[13-14] The conformation does not change upon dimer formation[15] or in the solid state.[5, 13] It is also very similar to that of cyclo(LPhe-DPhe).[14, 16] Cyclo(Tyr-Tyr) differs from cyclo(LPhe-LPhe) by the presence of the hydroxyl substituent in the benzene ring. This substituent leads to additional *syn*/*anti* isomerism,[17-18] and makes the formation of an OH…O hydrogen bond possible. Conformer-selective IR-UV spectroscopy showed that, besides the folded-extended conformation common to the two diastereomers, a stacked conformation stabilised by an OH…O interaction exists for cyclo(LTyr-LTyr) only.[19] Gas-phase cyclo(LTyr-LPhe) does not show this stacked geometry, although its existence was suggested in polar solvents.[20] The OH…π interaction is therefore not sufficient to counterbalance the strong repulsion between aromatic clouds.

Protonated cyclic dipeptides have been the subject of several studies, as possible intermediates in the fragmentation of peptides.[21-24] Comparison between collision-induced dissociation (CID) experiments and chemical dynamics simulations showed that the fragmentation processes of the amide CO protonated systems does not depend much on chirality, in contrast to those that are protonated on the side chain of a basic residue.[25-28] Protonation modifies the balance between the different conformers of biomolecules.[29] For cyclic dipeptides based on Tyr, Phe, or Pro residues, the proton is located on the amide CO and does not influence much its conformation. The extended conformation of protonated cyclo(Tyr-Pro) is dominant in a room-temperature ion trap, although minor amounts of folded conformers are kinetically trapped.[26] The most stable form of protonated cyclo(Phe-Phe) is similar for the two diastereomers and is a folded-extended geometry stabilized by an OH^+…π interaction.[28] This is the dominant species observed in protonated ions produced by electrospray ionisation (ESI) at room temperature. However, correct assignment of the vibrational spectrum requires the presence of higher-energy conformers resulting from kinetic trapping. They involve an NH…π interaction and are suggested to be responsible for the differences between the spectra of cyclo(LPhe-LPhe) and cyclo(LPhe-DPhe).[28] However, the spectral broadening due to spectral congestion and temperature effects prevents drawing a clear-cut conclusion. Low-temperature studies are therefore highly desirable for trapping the low-energy species and evidence their contribution to the stereochemistry-dependent spectroscopic results. Cryogenic ion traps are a powerful tool to stabilise and isolate small or medium-size peptides and study their structure by diverse action spectroscopy such as Infra-Red or Ultra-Violet Photodissociation (IRPD or UVPD), or a combination of both that results in

conformer-specific spectroscopy.[30-38] We apply here UVPD and IRPD to the study of protonated cyclo(Tyr-Tyr) in a cryogenic ion trap. The aim of this study is twofold. It aims first to test whether higher-energy conformers are necessary for observing a chirality effect in the vibrational spectroscopy of this molecule or if an effect is already observed at low temperature for the lower-energy conformer. On the other hand, the stereochemical effects observed in the neutral system rest on the presence of an OH…O hydrogen bond that can be formed in the cyclo(LTyr-LTyr) conformer only. The second aim of this work is thus to study the influence of the perturbation due to the excess charge (proton). The question that should be answered is whether the strong electrostatic interaction hides the chiral discrimination effect or if it is still visible in the most stable conformer of the two diastereomers of protonated cyclo(Tyr-Tyr), namely cyclo (LTyr-LTyr)H^+ and cyclo (LTyr-DTyr)H^+. They are denoted c-LLH^+ and c-LDH^+ in what follows and shown in Figure 1.

Material and methods

Experiment

Cyclo Tyr-Tyr(>99%) was purchased from Genecust (Luxembourg), and used without further purification. The experimental set-up has already been described in detail.[39] Briefly, the methanol solutions containing cyclo(Tyr-Tyr) at a concentration of 1.2×10^{-5} ML^{-1} with 0.5% of formic acid were electrosprayed from a nebuliser to generate fine droplets containing the target molecule. The droplets were evaporated by travelling through a glass capillary heated up to 70°C. The ions efficiently collected by an ion funnel were injected into a quadrupole mass spectrometer (Q-MS: Extrel) via a hexapole ion guide. The target molecule was mass-selected by the Q-MS and then introduced to a cryogenic quadrupole ion trap (QIT) via a quadrupole ion bender and octopole ion guide. The QIT was kept at 4K by a closed-cycle two-stage He cryostat (Sumitomo: RDK-408D2) during the whole experiment. A mixed buffer gas of H_2 (20%) and helium was introduced to the QIT using a pulsed valve (Parker Hannifin: General Valve Series 9). The mass-selected ions were allowed to collide with the cold buffer gas so that they were trapped in the QIT and cooled down to ~10K. The collision-induced dissociation (CID) experiments were performed in the QIT. The collision energy with He buffer gas was increased by increasing the kinetic energy of the ions injected into the QIT. The CID fragments were detected by a linear time-of-flight mass spectrometer (TOF-MS). For the IR spectroscopy, H_2 molecules were allowed to weakly attach to the ions under such cryogenic conditions.[40] The H_2-tagged ions were irradiated in the cold trap with a tunable IR laser (LaserVision: OPO/OPA). Hydrogen molecules were detached from the cluster ions when the wavenumber of the IR laser was resonant with a vibrational transition of the cluster ions.[41-42] The photofragments were extracted linearly and detected by the linear TOF-MS. The photofragment ion signals from a dynode converter detector of TOFMS were amplified 10 times by a preamplifier and recorded on a fast digitizer. IR photodissociation (IRPD) spectra were measured by monitoring the intensity of the photofragments (m/z 327) resulting from H_2 loss as a function of the wavenumber of the IR laser. IR-UV double resonance spectroscopy was performed to discuss the effect of H_2 tagging. UV photodissociation spectra were measured by monitoring the photofragments resulting from photoexcitation by a UV dye laser (Lumonics). IR-UV ion dip spectroscopy was not possible due to the broad nature of the UV

bands. The IR-UV enhanced spectra was measured instead. In this method, the UV wavenumber was fixed to the absorption maximum of the broad UV band. The tunable IR laser illuminated the ions of interest ~50 ns prior to the UV irradiation. The photofragment yield was enhanced by opening an additional fragmentation channel from the states populated by the electronic transition from vibrationally-excited states populated by IR absorption. The IR-UV enhanced spectrum is totally free from tag molecules.

Theoretical method

The structures of the protonated species, cyclo(LTyr-LTyr)H^+ and cyclo(LTyr-DTyr)H^+ were optimised in the framework of the density functional theory (DFT) using the B3LYP-D3 functional and the 6-311++G(d,p) basis sets.[43-45] All the calculations were performed with the Gaussian16 B01 software.[46] The frequencies were calculated at the same level of theory and scaled by 0.952 to account for anharmonicity and basis set incompleteness. The calculation level was chosen identical to that used for the study of the neutral molecule.[19] The scaling factor was the same as for the neutral molecule.[19] The potential energy surface was manually explored by building two types of initial structures in a systematic way. The first structures were built from the stable forms of protonated cyclo(PhePhe) modified by adding an hydroxyl substituent to the benzene ring, as it was successfully done before for finding the geometries of jet-cooled cyclo(Tyr-Phe) by removing an hydroxyl from neutral cyclo(Tyr-Tyr).[28] [47] To ensure that the exploration of the PES was complete, additional structures were obtained by adding a proton to the amide nitrogen or oxygen atom of the stable calculated structures of neutral cyclo(TyrTyr).[19] The structures whose vibrational spectrum shows the best match with the experiment were re-optimised at the B3LYP-D3(BJ) level. D3(BJ) dispersion correction have indeed proved to yield better structures for systems containing two aromatic rings like cyclophane.[48] In what follows, the energetics and structures are those obtained at the B3LYP-D3 level. Those at the B3LYP-D3(BJ) level are very similar and we shall only emphasise the differences in calculated frequencies.

Results

1) Theoretical results

Nomenclature: The conformational diversity of protonated cyclo(Tyr-Tyr) arises first from the orientation of the substituents, which in turn makes the protonation sites (CO or NH) non-equivalent. As described for the neutral molecule, each aromatic ring can take three possible orientations: two *gauche* and one *trans* forms, denoted as g^+, g^- and t, respectively. They correspond to dihedral angles τ(NCCC) of around 60°, -60° and 180°, respectively, for the L residue, with opposite values for the D residue. The g^+ geometry corresponds the aromatic substituent folded over the DKP ring while the g^- geometry corresponds to an aromatic ring extended outwards; these geometries are frequently encountered for neutral DKP peptides.[4, 13] The *trans* geometry corresponds to an aromatic ring extended outwards with an aromatic plane almost perpendicular to the peptide ring (see Figure 3). Moreover, the phenol OH can adopt two orientations that cannot be distinguished by their IR spectra.[12, 19, 33, 39, 49-50] We will therefore think in terms of “families” including both orientations of the OH bond.

The nomenclature used here rests on the geometry of the substituents and the nature of the protonation site, in the following way: each structure will be called c-LLH$^+$(AB_i) or c-LDH$^+$(AB_i) with A and B denoting the g^+, g^- or t geometry and i the protonation site, O or N, denoted in subscript of the corresponding residue.

Calculated structures: Four protonation sites are identified for c-LLH$^+$ and LDH$^+$, namely the CO and NH groups of each amide function. Protonation on NH results in conformers much higher in energy than protonation on CO. As shown for the related cyclo(Phe-Phe) protonated system, this difference is of the order of ~50 kJ mol^{-1}. We shall therefore limit the discussion to the species protonated on the amide CO. The energetic data are collected in Table 1. Because the distribution of conformers probably reflects a temperature between that of the electrospray and that of the ion trap, Table 1 gives the Gibbs free energies ΔG at room temperature (298 K) and at 350 K, together with the ZPE-corrected energies at 0 K. Unless specified otherwise, the energetic values given in what follows are ΔG at 298 K. All the calculated structures and energetic data, including those protonated on the amide NH, are shown in Figures S1 and S2 of the Supporting Information (SI). Adding two hydroxyl substituents to the most stable protonated structures of cyclo(LPhe-LPhe) or cyclo(LPhe-DPhe) results to c-LLH$^+$(g^+t_O) and c-LDH$^+$ (g^+t_O), which are the most stable structures (see Table 1 and Figure 3). In these structures, one of the phenol ring is folded over the peptide ring, which allows a weak $C_\beta H\ldots\pi$ interaction, as observed in one of the stable neutral forms. The other ring is extended in *trans* geometry, with the aromatic plane perpendicular to the DKP ring, which results in a stabilising interaction between the OH$^+$ and the folded aromatic ring. The strength of the OH…π interaction is different in c-LLH$^+$ and c-LDH$^+$, as attested by the length of the OH bond, which is slightly shorter in c-LL (0.985 Å) than in c-LD (0.990 Å), reflecting a slightly longer distance between the proton and the centre of the aromatic ring (2.51 Å for c-LLH$^+$(g^+t_O) *vs.* 2.48 Å for c-LDH$^+$(g^+t_O)). The second most stable structures derived from c-LPheLPheH$^+$ and c-LPheDPheH$^+$ are c-LLH$^+$(g^-t_O) and c-LDH$^+$(g^-t_O) and are calculated at 9.5 and 8.1 kJ mol^{-1} relative to the most stable form, respectively. Decreasing the temperature disfavours the g^-t_O conformers. In terms of structure, they are fully extended and involve a weak NH…π interaction. Both families of structures are stabilised by the interaction between the OH$^+$ and the aromatic ring, which is facilitated by the *trans* position of the latter. The last two structures deduced from protonated c-LPheLPhe and c-LPheDPhe are c-LLH$^+$($g^-g^+_O$) and c-LLH$^+$($g_O^-g^+$) for c-LL and the equivalent diastereomer structures c-LD($g^-g^+_O$), c-LDH$^+$($g_O^-g^+$). These structures have one ring folded and the other one extended. They are identical to those obtained by adding a proton to the folded/extended conformer of the neutral form. They are less stable by ~25 -28 kJ mol^{-1} than the most stable form because the *gauche* geometry of the extended ring prevent the OH…π to be formed. Last, adding a proton to the stacked conformer of neutral c-LL $g_O^+g^+$ result in a structure energetically disfavoured by ~ 30 kJ mol^{-1}.

2) Collision-induced dissociation

The CID MS² spectra of c-LLH$^+$ and c-LD H$^+$ obtained in identical conditions are shown in Figure 2. The same fragmentation pattern is observed for the two diastereomers. CID is usually less sensitive to the structure of epimer peptides than other dissociation methods such as electron-capture[51] or radical-induced dissociation.[52] However, the result obtained here contrasts to the stereoselectivity observed in histidine-containing cyclic dipeptides.[25, 53]

Besides the intense parent peak at *m/z* 327, two main fragments appear at *m/z* 136 and *m/z* 107. These fragments, together with the weak *m/z* 91 peak, are characteristic of tyrosine-containing peptides.[54] The *m/z* 136 fragment corresponds to the immonium ion, frequently observed in CID or UV-induced dissociation of charged peptides.[54-56] The immonium ion of tyrosine was also observed in the CID spectrum of cyclo(Tyr-Pro)H^+.[26] The fragments at *m/z* 107 arises from the immonium ion[54] and corresponds to the $C_\alpha C_\beta$ cleavage resulting in the hydroxybenzyl radical cation $CH_2C_6H_4OH^+$. A minor peak at *m/z* 300 corresponds to HCN loss. A weak peak at *m/z* 221 is assigned to the protonated cyclo(Gly–Tyr) cation resulting from the $C_\alpha C_\beta$ cleavage (loss of p-quinomethane). The simultaneous observation of *m/z* 107 and *m/z* 221 suggests that the $C_\alpha C_\beta$ cleavage results in the possible location of the positive charge on either of the fragments. It should be noted here that the fragment resulting from CO loss (*m/z* 299) is indiscernible in the MS^2 spectrum, which contrasts to related systems like cyclo(Phe-Phe)H^+ or cyclo(Tyr-Pro)H^+ for which CO loss appears at low collision energy and is the dominant CID fragment in all the collision energy range studied. Intense peaks corresponding to sequential fragmentation after CO loss are also observed in the CID spectrum of cyclo(Tyr-Pro)H^+, whose counterpart is completely absent here. The effect of stereochemistry is very limited in the system studied here. The CID efficiency is only slightly higher for c-LDH$^+$, but with no modification of the fragmentation pattern.

3) Spectroscopic results and assignment

Experimental spectra: In what follows, we will discuss the IRPD spectra obtained by the messenger technique. The spectra of the two diastereomers are shown in Figure 4 and clearly differ from each other. They can be divided in three regions. The higher-energy region contains a single band at 3633 cm^{-1} and 3628 cm^{-1} for c-LLH$^+$ and c-LDH$^+$ respectively, assigned to the free phenol ν(OH), whose frequency is almost identical for the two diastereomers. The 3300-3500 cm^{-1} region contains two bands characteristic of the amide ν(NH). They appear at different frequencies for c-LLH$^+$ (3417 cm^{-1} and 3348 cm^{-1}) and c-LDH$^+$ (3412 cm^{-1} and 3375 cm^{-1}). Lastly, the low-energy region shows a broad and intense band characteristic of the protonated amide ν(OH$^+$), which appears a different frequencies for c-LLH$^+$ and c-LDH$^+$ (3190 cm^{-1} and 3079 cm^{-1}, respectively).

Assignment: The spectra are well accounted for by that simulated for the most stable species, c-LLH$^+$(g^+t_O) and c-LDH$^+$(g^+t_O). The free phenol ν(OH) is mostly independent of the diastereomer. It shows a ~10 cm^{-1} down shift relative to the neutral molecule, which is due to the effect of H_2 tagging (see below). A similar frequency was observed in protonated tyrosine or cyclo(Tyr-Pro).[18, 26, 50] The ν(NH) region is well reproduced too by the simulations. Although the relative intensity of the two ν(NH) transitions is not quantitatively reproduced, the simulations account for the weaker intensity of the ν(NH) localised on the neutral amide and their similar frequencies for the two diasteromers. They also account for a larger down shift of the ν(NH) localised on the protonated amide in the case of c-LLH$^+$. The same difference between c-LLH$^+$ and c-LDH$^+$ was observed in protonated cyclo(Phe-Phe). It should be mentioned here that both frequencies and absorption intensities are identical whether the D3 or D3(BJ) correction is used. Also the bound ν(OH$^+$) frequency is calculated at different frequencies for c-LLH$^+$ and c-LDH$^+$, reproducing the lower frequency observed for c-LDH$^+$,

which in turns reflect a stronger OH^+…π interaction. The downshift of the bound ν(OH^+) frequency is underestimated for both diastereomers, which is a deficiency of the currently used method for modes involved in strong hydrogen bonds.[57-58] However, the D3(BJ) correction performs slightly better in this respect by shifting the calculated value further down in energy, thus closer to the experimental value. With both D3 and D3(BJ) corrections, the smaller red shift of ν(OH) in c-LLH^+ relative to c-LDH^+ correlates well with the strength of the OH^+…π interaction, as reflected by the distance between the proton and the centre of the aromatic ring mentioned above.

Effect of H_2 tagging: To assess the effect of the H_2 tag on the vibrational spectrum, the IRPD spectra are compared to the corresponding IR-UV enhanced spectra. To this end, the UV spectrum of c-LLH^+ and c-LDH^+ were recorded and are shown in Figure S3 of the SI. Despite the low temperature of the trap, they are broad and do not show any structure. This strongly contrasts to the behaviour of protonated tyrosine, the UV spectrum of which is well structured under ion trap conditions.[37, 39, 59] This result points towards fast deactivation processes in the cyclic dipeptide relative to the protonated amino acid. Figure S4 shows the IR-UV enhanced spectrum recorded by setting the UV wavelength at the maximum of the broad absorption. The band shifts induced by H_2 tagging are smaller than 10 cm^{-1} for the amide ν(NH) stretch, but the shifts are slightly larger for the phenol ν(OH) stretch (11-13 cm^{-1}). The largest shift (~30 cm^{-1}) is observed for the protonated ν(OH^+). However, the spectral patterns themselves did not change significantly, in agreement with recent results suggesting that H_2 tagging only perturbs the spectrum for highly symmetrical systems such as CH_5^+.[60] It should be noted that the ν(OH^+) is up-shifted by the H_2 tag, in contrast to the other modes that are down shifted. Moreover, the two phenolic ν(OH) undergo similar upshift upon tagging, as do the two amide ν(CH). These observations suggest the presence of an H_2 molecule on each aromatic ring in the tagged species. This hypothesis has been checked by measuring the mass spectrum of c-LLH^+ in the absence of the IR laser. It is shown in Figure S5 of the Supplementary Information. A strong peak appears at *m/z* 331, assigned to c-$LLH^+(H_2)_2$.

A very weak band is experimentally observed at 3551 cm^{-1} for both diastereomers. In addition, a very weak band appears for c-LDH^+ at ~3340 cm^{-1}. These bands could be due to an additional conformer kinetically trapped in our experimental conditions. The calculated spectrum of c-$LDH^+(g^-g^+_O)$ accounts well for the additional bands observed in the spectrum of c-LDH^+, with a band at 3551 cm^{-1} assigned to the free ν(OH^+).[28] The band at 3340 cm^{-1} would correspond to ν(NH), slightly shifted down in frequency due to the NH…π interaction. However, c-$LD(g^-g^+_O)$ is not the most stable c-$LD(g^-g^+)$ structure, and is 31.7 kJ mol^{-1} higher than c-$LD(g^-_Og^+)$. The spectrum of c-LLH^+ only shows the additional band at 3551 cm^{-1}, which could be due to c-$LL(g^+g^+_O)$ or c-$LL(g^-_Og^+)$. These two structures have relative Gibbs energy of +25.3 kJ mol^{-1} for c-$LL(g^-_Og^+)$ and +29.5 kJ mol^{-1} for c-$LL(g^+g^+_O)$. Although the corresponding structures are among the most stable for cyclo (Phe-Phe)H^+ and contribute to its IRMPD spectrum at room temperature, their contribution here is expected to be very limited due to the low temperature of the trap. We therefore conclude that these bands are due to species complexed by more than two H_2 tags. The weak band at 3551 cm^{-1} could be due to a species in which an additional H_2 molecule attaches to one of the phenol OH. The band at 3340 cm^{-1} could be due to a species in which an additional H_2 molecule attaches to one of the amide NH.

The most stable structures of c-LLH$^+$ and c-LDH$^+$ are similar to those calculated for protonated cyclo(Phe-Phe), and so are the spectra simulated at the same level of calculations. The ν(OH$^+$) frequency is shifted down by 110 cm^{-1} in c-LDH$^+$ and appears at 3079 cm^{-1} for LD *vs.* 3190 cm^{-1} for LL. This difference in frequency was calculated also in cyclo(Phe-Phe)H$^+$ but was difficult to observe experimentally due to the experimental conditions at room temperature resulting in broad transitions.

Conclusion

The structure responsible for the experimentally observed spectrum is the most stable calculated form, for c-LLH$^+$ and c-LDH$^+$ alike. The most stable c-LLH$^+$ structure is more stable than the most stable c-LDH$^+$ by 1.77 kJ mol^{-1}. Although very small, probably within the error of the calculation, this energy difference parallels the CID efficiency, which is slightly larger for c-LDH$^+$. The effect of the charge is dominant in these systems and protonation induces a dramatic change in the structure, preventing the formation of the stacked geometry observed in the neutral molecule for c-LL. However, the chiral selection overcomes the strong perturbation induced by the excess charge and a clear difference is observed in the IRPD spectra of the two diastereomers. The cold temperature achieved here minimises the presence of higher-energy conformers in contrast to the room temperature experiments[61] and makes it possible to evidence the differences in the ν(OH$^+$) and protonated amide ν(NH) stretch frequencies between the two diastereomers. These results confirm that the chirality effects are visible in the most stable structure of protonated cyclic peptides.

Supporting Information.

Calculated structures and simulated spectra for the structures not discussed in the main text. UVPD spectra. Comparison between H_2 tagging and IR-UV enhanced spectroscopy results.

Acknowledgments

A.Z. acknowledges travel support from the World Research Hub Initiative (WRHI) of Tokyo Institute of Technology. This work was supported in part by KAKENHI (JP19K23624, JP20K20446, JP20H00372, JP21H04674, and JP21K14585) of JSPS, World Research Hub Initiatives in Tokyo Institute of Technology, the Cooperative Research Program of the "Network Joint Research Centre for Materials and Devices" and Core-to-core program (JPJSCCA20210004) from the Ministry of Education, Culture, Sports, Science and Technology (MEXT), Japan, and the RIKEN Pioneering Project, "Fundamental Principles Underlying the Hierarchy of Matter: A Comprehensive Experimental Study". The computations were performed at the Research Centre for Computational Science, Okazaki, Japan (21-IMS-C109).

Structure name	ΔG/ KJ mol^{-1} @298K	ΔG/ KJ mol^{-1} @350K	ZPE-corrected ΔG/ KJ mol^{-1}	Structure name	ΔG/ KJ mol^{-1} @298K	ΔG/ KJ mol-1 @350K	ZPE-corrected ΔG/ KJ mol^{-1}
c-LL(g^+t_O)	0.0	0.0	0.0	c-LD(g^+t_O)	0.0	0.0	0.0
c-LL(g^-t_O)	9.5	8.5	14.4	c-LD(g^-t_O)	8.1	6.0	18.7
c-LL($g^-_Og^+$)	25.3	25.2	25.7	c-LD($g^-g^+_O$)	20. 3	19.3	25.4
c-LL(g^-t_O)	28.0	26.5	35.6	c-LD($g^-_Og^-$)	23. 3	21.0	34.5
c-LL(g^-_Ot)	28.0	26.5	35.6	c-LD($g^-g^-_O$)	24.9	22.6	35.8
c-LL($g^+g^+_O$)	29.5	30.3	25.5	c-LD($g^-_Og^-$)bis	28.2	26.0	38.5
c-LL($g^-g_O{}^+$)	31.4	31.4	30.9	c-LD($g^-g^-_O$)bis	29.3	27.0	40.0
c-LL(g^-_Ot)	33.1	31.6	40.7	c-LD($g^-g^+_O$)	31.7	30.7	36.5
c-LL($g^-_Og^-$)	40.5	39.2	46.7	c-LD(g^-_Ot)	34.9	32.7	45.5
c-LL($g^+g^+_N$)	52.1	52.7	48.7	c-LD(g^-t) bis	46.7	44.0	60.0
c-LL($g^-g^+_N$)	69.1	69.0	69.3	c-LD($g^-_N g^+$)	51.4	49.6	59.8
c-LL($g^-g^+_N$)	73.9	73.5	76.1	c-LD(g^-t) ter	55.7	53.2	67.3
				c-LD($g^-g^+_N$)	68.9	67.0	78.7

Table 1: Energetic data for the most stable calculated structures of c-LLH$^+$ and c-LDH$^+$

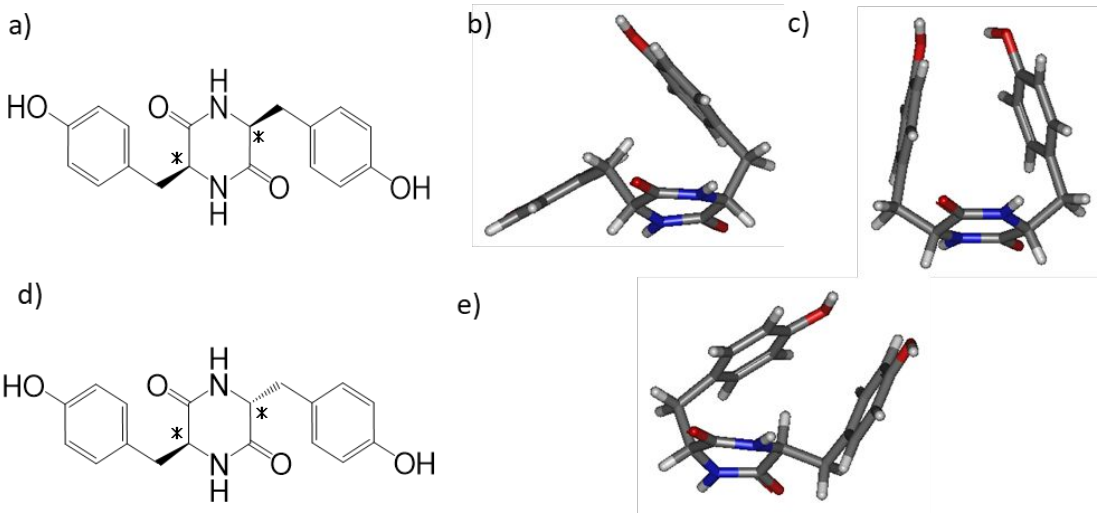

Figure 1: Scheme of the studied molecules and structures observed in the gas phase. The chiral centres are indicated by *. a) Schematic view of the homochiral neutral dipeptide c-LL. b) and c) observed structures for neutral c-LL. d) Schematic view of the heterochiral neutral dipeptide c-LD. e) observed structure for neutral c-LD. Note that the stacked structure (c) is only observed for c-LL.

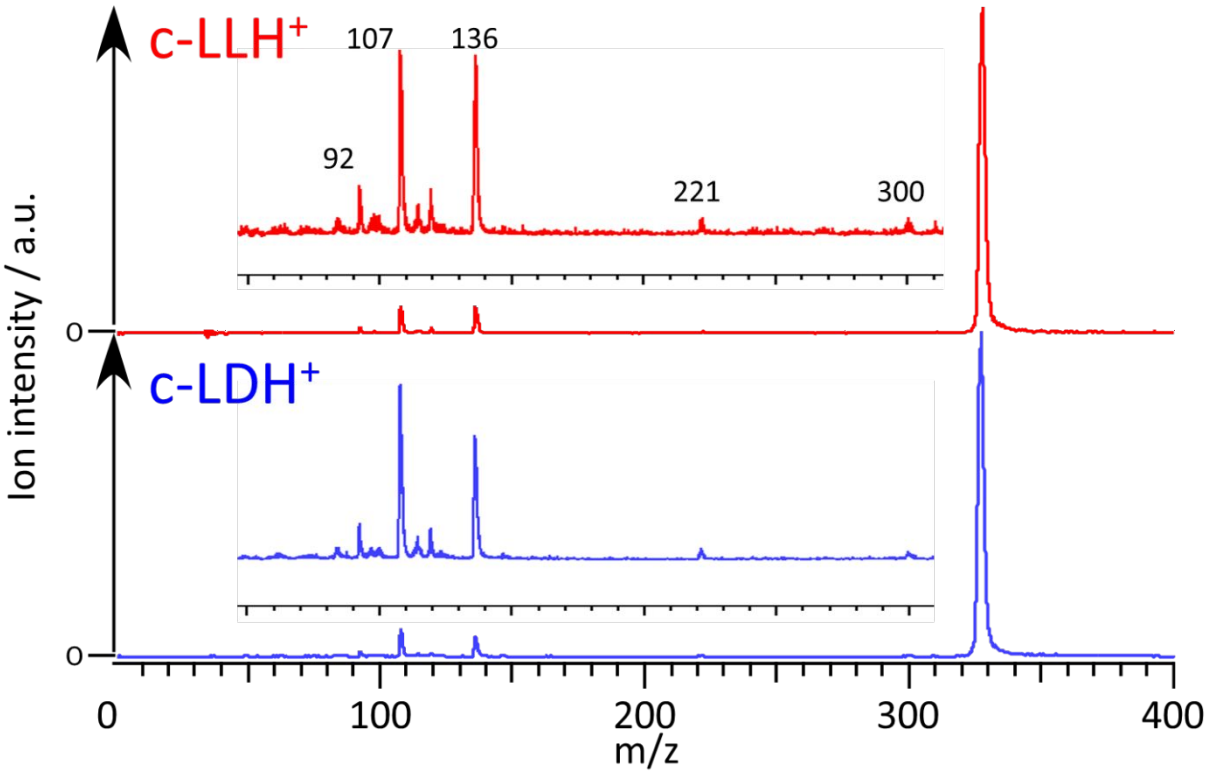

Figure 2: MS^2 spectrum obtained by collision-induced dissociation of the parent *m/z* 327 for the protonated diastereoisomers of cyclo(Tyr-Tyr) $cLLH^+$ (top) and $c\text{-}LDH^+$ (bottom).

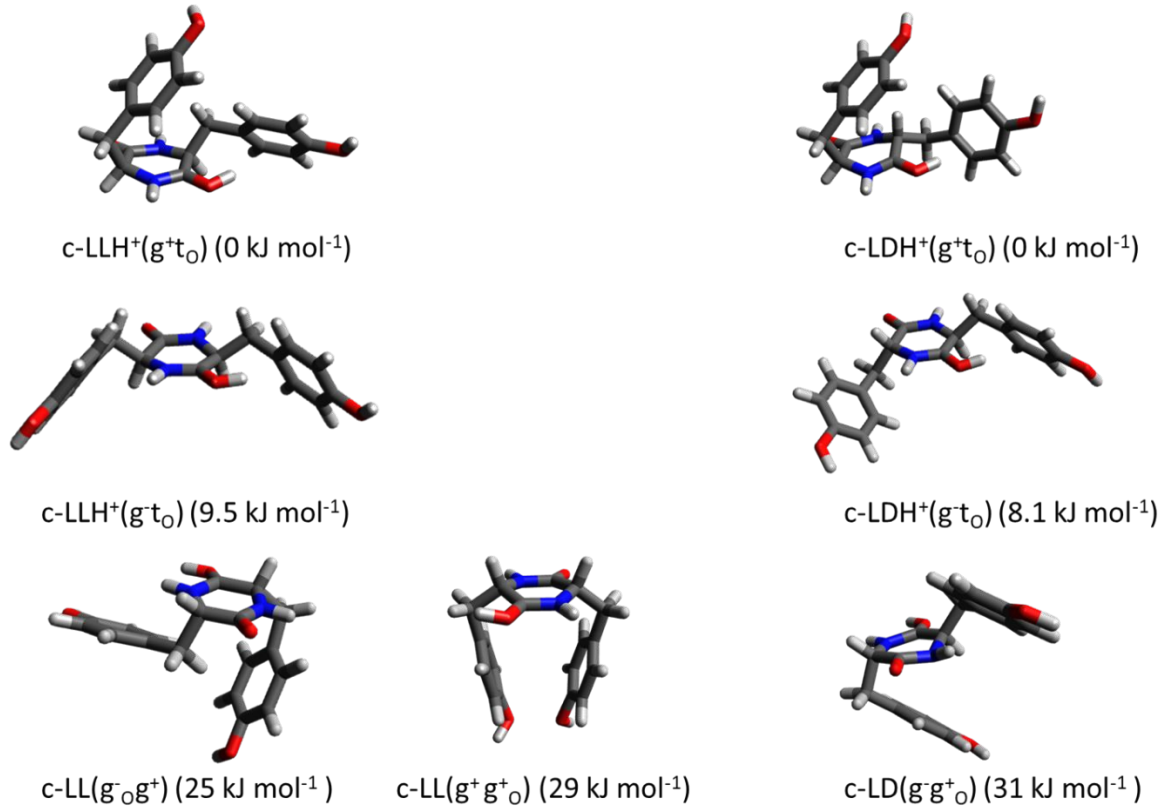

Figure 3: Most stable calculated structures of the protonated diastereoisomers of cyclo(Tyr-Tyr) c-LLH$^+$ (left) and c-LDH$^+$ (right).

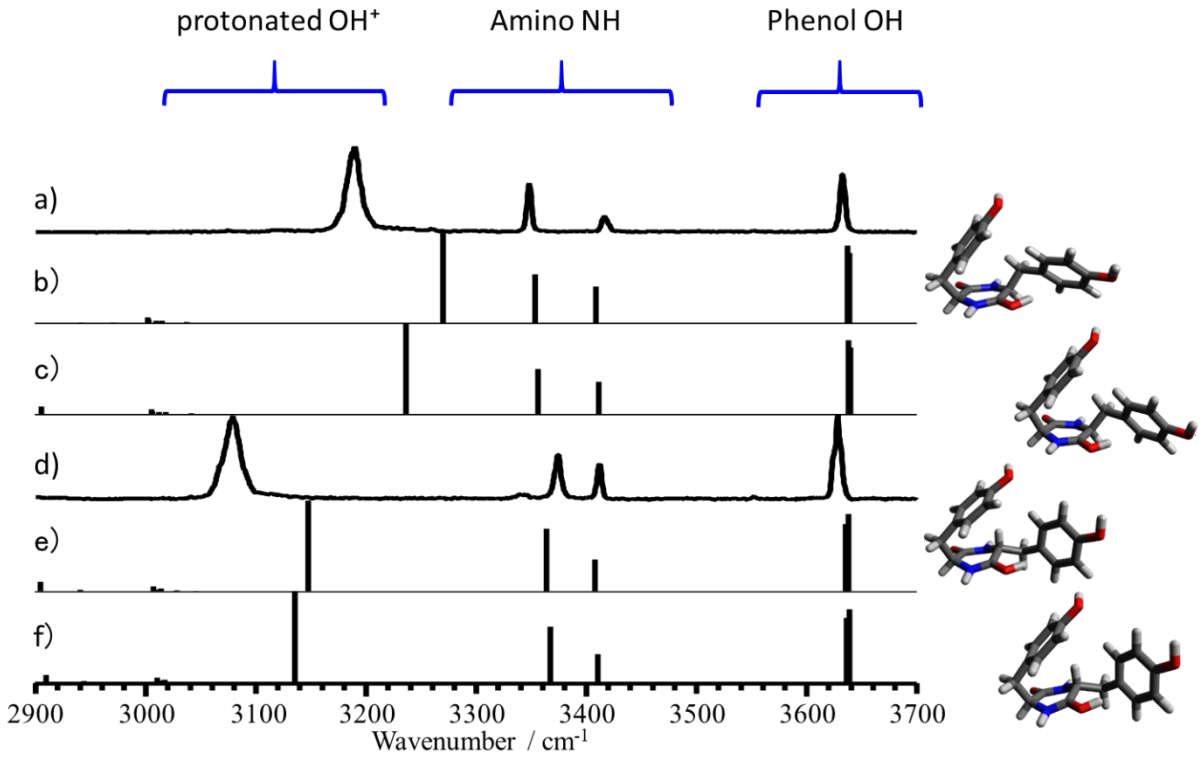

Figure 4: Comparison between the experimental spectra of (a) c-LLH$^+$ and (d) c-LDH$^+$ and those calculated for the most stable structures: (b) c-LLH$^+$(g^+t_O) at the B3LYP-D3/6-311++g(d,p) level of theory. (c) Same with D3BJ dispersion correction. (e) c-LDH$^+$(g^+t_O) at the B3LYP-D3/6-311++g(d,p) level of theory. (f) Same with D3BJ dispersion correction. The frequencies have been scaled by 0.952 (see text).

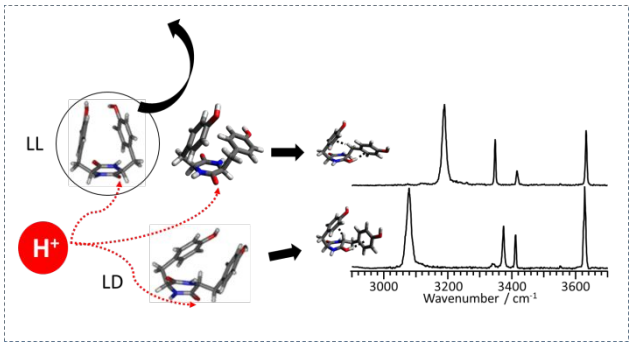

Graphical Abstract for TOC

References

1. Borthwick, A. D., 2,5-Diketopiperazines: Synthesis, Reactions, Medicinal Chemistry, and Bioactive Natural Products. *Chemical Reviews* **2012,** *112* (7), 3641-3716.

2. Balachandra, C.; Padhi, D.; Govindaraju, T., Cyclic Dipeptide: A Privileged Molecular Scaffold to Derive Structural Diversity and Functional Utility. *Chemmedchem* **2021,** *16* (17), 2558-2587.
3. Carlson, K. L.; Lowe, S. L.; Hoffmann, M. R.; Thomasson, K. A., Theoretical UV circular dichroism of aliphatic cyclic dipeptides. *Journal of Physical Chemistry A* **2005,** *109* (24), 5463-5470.
4. Milne, P. J.; Oliver, D. W.; Roos, H. M., Cyclodipeptides - Structure and Conformation of Cyclo(Tyrosyl Prolyl). *Journal of Crystallographic and Spectroscopic Research* **1992,** *22* (6), 643-649.
5. Gdaniec, M.; Liberek, B., Structure of Cyclo(-L-Phenylalanyl-L-Phenylalanyl-). *Acta Crystallographica Section C-Crystal Structure Communications* **1986,** *42*, 1343-1345.
6. Strickland, E. H.; Wilchek, M.; Horwitz, J.; Billups, C., Low Temperature Circular Dichorism of Tyrosyl and Tryptophanyl Diketopiperazines. *Journal of Biological Chemistry* **1970,** *245* (16), 4168-+.
7. Yamazaki, T.; Saidnejad, O. E.; Schiller, P. W.; Goodman, M., Conformational Studies of Stereoisomeric 14-Membered Cyclic Enkephalin Analogs Containing 1-Naphthylalanine at the 4th Position - Chirality Effect of Leucine at the 5th Position on Biological-Activity and Receptor Selectivity. *Biopolymers* **1991,** *31* (7), 877-898.
8. Bettens, F. L.; Bettens, R. P. A.; Brown, R. D.; Godfrey, P. D., The microwave spectrum, structure, and ring-puckering of the cyclic dipeptide diketopiperazine. *Journal of the American Chemical Society* **2000,** *122* (24), 5856-5860.
9. Kopple, K. D.; Marr, D. H., Conformation of cyclic peptides. The folding of cyclic dipeptides containing an aromatic side chain. *Journal of the American Chemical Society* **1967,** *89* (24), 6193-200.
10. Lin, C.-F.; Webb, L. E., Crystal structures and conformations of the cyclic dipeptides cyclo-(Glycyl-L-tyrosyl) and cyclo-(L-seryl-L-tyrosyl) Monohydrate. *Journal of the American Chemical Society* **1973,** *95* (20), 6803-11.
11. Wiedemann, S.; Metsala, A.; Nolting, D.; Weinkauf, R., The dipeptide cyclic(glycyltryptophanyl) in the gas phase: A concerted action of density functional calculations, S-0-S-1 two-photon ionization, spectral UV/UV hole burning and laser photoelectron spectroscopy. *Physical Chemistry Chemical Physics* **2004,** *6* (10), 2641-2649.
12. Pérez-Mellor, A.; Alata, I.; Lepère, V.; Zehnacker, A., Conformational Study of the Jet-Cooled Diketopiperazine Peptide Cyclo Tyrosyl-Prolyl. *The Journal of Physical Chemistry B* **2019,** *123* (28), 6023-6033.
13. Pérez Mellor, A.; Zehnacker, A., Chirality Effects in Jet-Cooled Cyclic Dipeptides. In *Physical Chemistry of Cold Gas-Phase Functional Molecules and Clusters*, Ebata, T.; Fujii, M., Eds. Springer: Singapore, 2019; pp 63-87.
14. Pérez-Mellor, A.; Alata, I.; Lepere, V.; Zehnacker, A., Chirality effects in the structures of jet-cooled bichromophoric dipeptides. *Journal of Molecular Spectroscopy* **2018,** *349*, 71-84.
15. Bakels, S.; Gaigeot, M. P.; Rijs, A. M., Gas-Phase Infrared Spectroscopy of Neutral Peptides: Insights from the Far-IR and THz Domain. *Chemical Reviews* **2020,** *120* (7), 3233-3260.
16. Pérez-Mellor, A.; Zehnacker, A., Vibrational circular dichroism of a 2,5-diketopiperazine (DKP) peptide: Evidence for dimer formation in cyclo LL or LD diphenylalanine in the solid state. *Chirality* **2017,** *29* (2), 89-96.
17. Inokuchi, Y.; Kobayashi, Y.; Ito, T.; Ebata, T., Conformation of L-tyrosine studied by fluorescence-detected UV-UV and IR-UV double-resonance spectroscopy. *Journal of Physical Chemistry A* **2007,** *111* (17), 3209-3215.
18. Shimozono, Y.; Yamada, K.; Ishiuchi, S.; Tsukiyama, K.; Fujii, M., Revised conformational assignments and conformational evolution of tyrosine by laser desorption supersonic jet laser spectroscopy. *Physical Chemistry Chemical Physics* **2013,** *15* (14), 5163-5175.
19. BenNasr, F.; Pérez-Mellor, A.; Alata, I.; Lepere, V.; Jaidane, N. E.; Zehnacker, A., Stereochemistry-dependent hydrogen bonds stabilise stacked conformations in jet-cooled cyclic dipeptides: (LD) vs. (LL) cyclo tyrosine-tyrosine. *Faraday Discussions* **2018,** *212*, 399-419.
20. Yamazaki, T.; Nunami, K. I.; Goodman, M., Cyclic Retro-Inverso Dipeptides with 2 Aromatic Side-Chains .2. Conformational-Analysis. *Biopolymers* **1991,** *31* (13), 1513-1528.

21. Wang, D.; Gulyuz, K.; Stedwell, C. N.; Polfer, N. C., Diagnostic NH and OH Vibrations for Oxazolone and Diketopiperazine Structures: b(2) from Protonated Triglycine. *Journal of the American Society for Mass Spectrometry* **2011,** *22* (7), 1197-1203.
22. Oomens, J.; Young, S.; Molesworth, S.; van Stipdonk, M., Spectroscopic Evidence for an Oxazolone Structure of the b(2) Fragment Ion from Protonated Tri-Alanine. *Journal of the American Society for Mass Spectrometry* **2009,** *20* (2), 334-339.
23. Perkins, B. R.; Chamot-Rooke, J.; Yoon, S. H.; Gucinski, A. C.; Somogyi, A.; Wysocki, V. H., Evidence of Diketopiperazine and Oxazolone Structures for HA b(2)($^{+}$) Ion. *Journal of the American Chemical Society* **2009,** *131* (48), 17528-17529.
24. Shek, P. Y. I.; Lau, J. K.-C.; Zhao, J.; Grzetic, J.; Verkerk, U. H.; Oomens, J.; Hopkinson, A. C.; Siu, K. W. M., Fragmentations of protonated cyclic-glycylglycine and cyclic-alanylalanine. *International Journal of Mass Spectrometry* **2012,** *316*, 199-205.
25. Pérez-Mellor, A.; Le Barbu-Debus, K.; Lepere, V.; Alata, I.; Spezia, R.; Zehnacker, A., Structure and collision-induced dissociation of the protonated cyclo His-Phe dipeptide: mechanistic studies and stereochemical effects. *The European Physical Journal D* **2021,** *75* (6).
26. Pérez-Mellor, A.; Alata, I.; Lepère, V.; Spezia, R.; Zehnacker-Rentien, A., Stereospecific collision-induced dissociation and vibrational spectroscopy of protonated cyclo (Tyr-Pro). *International Journal of Mass Spectrometry* **2021,** *465*.
27. Pérez Mellor, A.; Spezia, R., Determination of kinetic properties in unimolecular dissociation of complex systems from graph theory based analysis of an ensemble of reactive trajectories. *The Journal of Chemical Physics* **2021,** *155*.
28. Alata, I.; Pérez-Mellor, A.; Ben Nasr, F.; Scuderi, D.; Steinmetz, V.; Gobert, F.; Jaïdane, N. E.; Zehnacker-Rentien, A., Does the Residues Chirality Modify the Conformation of a Cyclo-Dipeptide? Vibrational Spectroscopy of Protonated Cyclo-diphenylalanine in the Gas Phase. *The Journal of Physical Chemistry A* **2017,** *121* (38), 7130-7138.
29. Rijs, A. M.; Oomens, J., *Gas-Phase IR Spectroscopy and Structure of Biological Molecules*. Springer International Publishing: 2015.
30. Ishiuchi, S.; Sasaki, Y.; Lisy, J. M.; Fujii, M., Ion-peptide interactions between alkali metal ions and a termini-protected dipeptide: modeling a portion of the selectivity filter in K+ channels. *Physical Chemistry Chemical Physics* **2019,** *21* (2), 561-571.
31. Thomas, D. A.; Marianski, M.; Mucha, E.; Meijer, G.; Johnson, M. A.; von Helden, G., Ground-State Structure of the Proton-Bound Formate Dimer by Cold-Ion Infrared Action Spectroscopy. *Angewandte Chemie-International Edition* **2018,** *57* (33), 10615-10619.
32. Leavitt, C. M.; Wolk, A. B.; Fournier, J. A.; Kamrath, M. Z.; Garand, E.; Van Stipdonk, M. J.; Johnson, M. A., Isomer-Specific IR-IR Double. Resonance Spectroscopy of D-2-Tagged Protonated Dipeptides Prepared in a Cryogenic Ion Trap. *Journal of Physical Chemistry Letters* **2012,** *3* (9), 1099-1105.
33. Stearns, J. A.; Guidi, M.; Boyarkin, O. V.; Rizzo, T. R., Conformation-specific infrared and ultraviolet spectroscopy of tyrosine-based protonated dipeptides. *Journal of Chemical Physics* **2007,** *127* (15), 154322.
34. Wako, H.; Ishiuchi, S.; Kato, D.; Feraud, G.; Dedonder-Lardeux, C.; Jouvet, C.; Fujii, M., A conformational study of protonated noradrenaline by UV-UV and IR dip double resonance laser spectroscopy combined with an electrospray and a cold ion trap method. *Physical Chemistry Chemical Physics* **2017,** *19* (17), 10777-10785.
35. Harrilal, C. P.; DeBlase, A. F.; McLuckey, S. A.; Zwier, T. S., Two-Color IRMPD Applied to Conformationally Complex Ions: Probing Cold Ion Structure and Hot Ion Unfolding. *Journal of Physical Chemistry A* **2021,** *125* (42), 9394-9404.
36. Soorkia, S.; Jouvet, C.; Gregoire, G., UV Photoinduced Dynamics of Conformer-Resolved Aromatic Peptides. *Chemical Reviews* **2020,** *120* (7), 3296-3327.
37. Soorkia, S.; Broquier, M.; Gregoire, G., Conformer- and Mode-Specific Excited State Lifetimes of Cold Protonated Tyrosine Ions. *Journal of Physical Chemistry Letters* **2014,** *5* (24), 4349-4355.

38. Lawler, J. T.; Harrilal, C. P.; DeBlase, A. F.; Sibert, E. L., III; McLuckey, S. A.; Zwier, T. S., Single-conformation spectroscopy of cold, protonated (D)PG-containing peptides: switching beta-turn types and formation of a sequential type II/II ' double beta-turn. *Physical Chemistry Chemical Physics* **2022,** *24* (4), 2095-2109.
39. Ishiuchi, S.; Wako, H.; Kato, D.; Fujii, M., High-cooling-efficiency cryogenic quadrupole ion trap and UV-UV hole burning spectroscopy of protonated tyrosine. *Journal of Molecular Spectroscopy* **2017,** *332*, 45-51.
40. Wang, X. B.; Xing, X. P.; Wang, L. S., Observation of H-2 Aggregation onto a Doubly Charged Anion in a Temperature-Controlled Ion Trap. *Journal of Physical Chemistry A* **2008,** *112* (51), 13271-13274.
41. Kamrath, M. Z.; Relph, R. A.; Guasco, T. L.; Leavitt, C. M.; Johnson, M. A., Vibrational predissociation spectroscopy of the H-2-tagged mono- and dicarboxylate anions of dodecanedioic acid. *International Journal of Mass Spectrometry* **2011,** *300* (2-3), 91-98.
42. Donon, J.; Bardaud, J.-X.; Brenner, V.; Ishiuchi, S.-I.; Fujii, M.; Gloaguen, E., Stepwise dissociation of ion pairs by water molecules: cation-dependent separation mechanisms between carboxylate and alkali-earth metal ions. *Physical chemistry chemical physics : PCCP* **2022**.
43. Becke, A. D., Density-functional exchange-energy approximation with correct asymptotic-behavior. *Physical Review A* **1988,** *38* (6), 3098-3100.
44. Halls, M. D.; Velkovski, J.; Schlegel, H. B., Harmonic frequency scaling factors for Hartree-Fock, S-VWN, B-LYP, B3-LYP, B3-PW91 and MP2 with the Sadlej pVTZ electric property basis set. *Theoretical Chemistry Accounts* **2001,** *105*, 413.
45. Frisch, M. J.; Pople, J. A.; Binkley, J. S., Self-Consistent Molecular-Orbital Methods .25. Supplementary Functions for Gaussian-Basis Sets. *Journal of Chemical Physics* **1984,** *80* (7), 3265-3269.
46. Frisch, M. J.; Trucks, G. W.; Schlegel, H. B.; Scuseria, G. E.; Robb, M. A.; Cheeseman, J. R.; Scalmani, G.; Barone, V.; Petersson, G. A.; Nakatsuji, H.; et al. *Gaussian 16 Rev. B.01*, Wallingford, CT, 2016.
47. Dupont, J.; Guillot, R.; Lepère, V.; Zehnacker, A., Jet-cooled laser spectroscopy and solid-state vibrational circular dichroism of the cyclo-(Tyr-Phe) diketopiperazine dipeptide. *Journal of Molecular Structure* **2022,** *1262*, 133059.
48. Grimme, S.; Muck-Lichtenfeld, C., Accurate Computation of Structures and Strain Energies of Cyclophanes with Modern DFT Methods. *Israel Journal of Chemistry* **2012,** *52* (1-2), 180-192.
49. Hirata, K.; Mori, Y.; Ishiuchi, S. I.; Fujii, M.; Zehnacker, A., Chiral discrimination between tyrosine and beta-cyclodextrin revealed by cryogenic ion trap infrared spectroscopy. *Physical Chemistry Chemical Physics* **2020,** *22* (43), 24887-24894.
50. Stearns, J. A.; Mercier, S.; Seaiby, C.; Guidi, M.; Boyarkin, O. V.; Rizzo, T. R., Conformation-specific Spectroscopy and photodissociation of cold, protonated tyrosine and phenylalanine. *Journal of the American Chemical Society* **2007,** *129* (38), 11814-11820.
51. Adams, C. M.; Kjeldsen, F.; Zubarev, R. A.; Budnik, B. A.; Haselmann, K. F., Electron capture dissociation distinguishes a single D-amino acid in a protein and probes the tertiary structure. *Journal of the American Society for Mass Spectrometry* **2004,** *15* (7), 1087-1098.
52. Tao, Y. Q.; Quebbemann, N. R.; Julian, R. R., Discriminating D-Amino Acid-Containing Peptide Epimers by Radical-Directed Dissociation Mass Spectrometry. *Analytical Chemistry* **2012,** *84* (15), 6814-6820.
53. Perez-Mellor, A. F.; Spezia, R.; Zehnacker, A., How Symmetry Influences the Dissociation of Protonated Cyclic Peptides. *Symmetry-Basel* **2022,** *14* (4).
54. Falick, A. M.; Hines, W. M.; Medzihradszky, K. F.; Baldwin, M. A.; Gibson, B. W., Low-mass ions produced from peptides by high-energy collision-induced dissociation in tandem mass-spectrometry. *Journal of the American Society for Mass Spectrometry* **1993,** *4* (11), 882-893.
55. Ambihapathy, K.; Yalcin, T.; Leung, H. W.; Harrison, A. G., Pathways to immonium ions in the fragmentation of protonated peptides. *Journal of mass spectrometry* **1997,** *32* (2), 209-215.

56. Madsen, J. A.; Boutz, D. R.; Brodbelt, J. S., Ultrafast Ultraviolet Photodissociation at 193 nm and its Applicability to Proteomic Workflows. *Journal of Proteome Research* **2010,** *9* (8), 4205-4214.
57. Rodrigues-Oliveira, A. F.; Ribeiro, F. W. M.; Cervi, G.; Correra, T. C., Evaluation of Common Theoretical Methods for Predicting Infrared Multiphotonic Dissociation Vibrational Spectra of Intramolecular Hydrogen-Bonded Ions. *Acs Omega* **2018,** *3* (8), 9075-9085.
58. Ben Nasr, F.; Alata, I.; Scuderi, D.; Lepere, V.; Brenner, V.; Jaïdane, N. E.; Zehnacker, A., Effects of complexation with sulfuric acid on the photodissociation of protonated Cinchona alkaloids in the gas phase. *Physical Chemistry Chemical Physics* **2019,** *21* (28), 15439-15451.
59. Boyarkin, O. V.; Mercier, S. R.; Kamariotis, A.; Rizzo, T. R., Electronic spectroscopy of cold, protonated tryptophan and tyrosine. *Journal of the American Chemical Society* **2006,** *128* (9), 2816-2817.
60. Esser, A.; Forbert, H.; Marx, D., Tagging effects on the mid-infrared spectrum of microsolvated protonated methane. *Chemical Science* **2018,** *9* (6), 1560-1573.
61. Zehnacker, A., Chirality Effects in Gas-Phase Spectroscopy and Photophysics of Molecular and Ionic Complexes: Contribution of Low and Room Temperature Studies. *International Reviews in Physical Chemistry* **2014,** *33* (2), 151-207.